

行政院原子能委員會  
委託研究計畫研究報告

頭部專用核醫造影系統之衰減校正方法研究與效能驗證

Investigation and performance evaluation of attenuation correction  
for dedicated brain PET system

計畫編號：108A015

受委託機關(構)：高雄醫學大學

計畫主持人：楊晴晴

聯絡電話：(07)3121101 分機 2356-51

E-mail address：cyang@kmu.edu.tw

研究期程：中華民國 108 年 8 月 29 日至 108 年 12 月 31 日

研究經費：新臺幣伍拾萬貳仟柒佰元整

核研所聯絡人員：張家豪

報告日期：108 年 12 月 15 日

## 目 錄

中文摘要.....	2
英文摘要.....	3
壹、計畫緣起與目的.....	5
貳、研究方法與過程.....	10
一、    深度學習模型 .....	10
二、    腦部 PET 成像系統之蒙地卡羅模擬 .....	12
三、    臨床病人腦部 PET/CT 掃描 .....	17
四、    工作項目與執行時程 .....	18
參、主要發現與結論.....	19
一、    研究結果 .....	19
二、    討論與建議 .....	25
三、    結論 .....	28
肆、參考文獻.....	30
附註.....	32

## 中文摘要

正子發射斷層掃描 (PET) 會因為互毀光子於病人體內衰減導致影像在視覺判讀和量化分析表現不佳，從而對核醫藥物活性分布的定量與定性產生不良影響，此一現象產生了在 PET 影像重建中實施衰減校正的需求。本案目標為探討在無需額外解剖成像的情況下對腦部 PET 影像以基於捲積神經網路 (CNN) 技術進行衰減校正的可行性，研究執行是由高雄醫學大學醫放系楊晴晴老師實驗室完成以下工作：

(1) 建立一套基於 GATE 為計算核心的蒙地卡羅模擬器，以對核能研究所設計的腦部 PET 系統進行建模；(2) 完成 198 組的 PET 模擬掃描運算以訓練和測試 CNN 模型；(3) 研究計畫送交台大醫院臨床試驗審查委員會 (IRB) 審議並獲得批准；(4) 收集 20 組臨床病人腦部 PET/CT 掃描以訓練和測試 CNN 模型；(5) 建立了基於 Caffe 為演算平台的深度學習環境；(6) 探討一種 CNN 模型於實現 PET 衰減校正的表現情形。本案所採用的 CNN 模型，其輸出數據與標籤數據仍有很大差異。然而我們從這些初步結果發現，為了成功訓練深度學習模型於實現 PET 衰減校正，可從模擬腦部數位假體、增加訓練數據量和加深 CNN 模型的結構上修正。本案所獲得的研究結果與衍生建議將有助於開發基於深度學習法的 PET 衰減校正技術。

## 英文摘要

Attenuation of photons in vivo degrades the visual quality and quantitative accuracy of PET images, thereby adversely affecting interpretation and quantitation of activity concentration. Accurate attenuation correction is therefore mandatory in quantitative PET image reconstruction. This study aimed to investigate the feasibility of attenuation correction based on convolutional neural network (CNN) technique in brain PET imaging without additional anatomical imaging. To achieve this goal, our members from Dr. Ching-Ching Yang's Lab at Kaohsiung Medical University have accomplished the following works: (1) a Monte Carlo simulator based on GATE has been built to model the brain PET system designed by Institute of Nuclear Energy Research; (2) 198 simulations have been conducted to train and test the CNN model; (3) institutional review board approval issued by National Taiwan University Hospital was obtained; (4) 20 real PET/CT scans were collected to train and test the CNN model; (5) a deep learning environment based on Caffe has been set up; (6) a CNN model has been investigated for estimating attenuation corrected PET from uncorrected PET. Although the output data from the investigated CNN model have large discrepancy from the label data, these preliminary results give us valuable information concerning the simulation phantom type, the training data size, and the architecture of the CNN model. It is believed that the performance of the deep learning based attenuation correction for brain PET imaging can be substantially improved once the suggested

modifications have been made.

## Investigation and performance evaluation of attenuation correction for dedicated brain PET system

Ching-Ching Yang, Ph.D.

Department of Medical Imaging and Radiological Sciences,  
Kaohsiung Medical University

### 壹、計畫緣起與目的

As worldwide health improvements have increased, life expectancy increases but neurodegenerative disorders become more common.  $^{18}\text{F}$ -FDG PET is not only a valuable tool in tumor imaging but also a very promising neuroimaging tool in the diagnosis of neurodegenerative disease because it reflects resting state cerebral metabolic rates of glucose, which is an indicator of neuronal activity (Fig. 1). Indications of dementing disorders include early diagnosis and differential diagnosis of dementing disorders, such as Alzheimer's disease and frontotemporal dementia. Typical topographic patterns of hypometabolism may help diagnose the main neurodegenerative diseases at a predementia stage, i.e.,

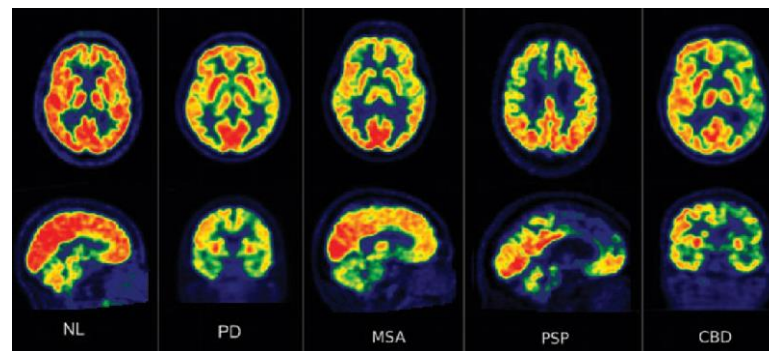


Fig. 1.  $^{18}\text{F}$ -FDG PET scans of a representative cognitive normal individual (NL, left) and of four patients, each with a different movement disorder (from left to right): Parkinson's disease (PD), multiple system atrophy (MSA), progressive supranuclear palsy (PSP), and corticobasal degeneration (CBD).<sup>1</sup>

mild cognitive impairment.  $^{18}\text{F}$ -FDG PET can also be used in differential diagnosis of cerebral space-occupying lesions, detection of viable tumor tissue and for noninvasive grading. As for epilepsy, a common indication is the preoperative evaluation of partial epilepsy in adults and in children to identify the functional deficit zone. With regards to movement disorders,  $^{18}\text{F}$ -FDG PET can be used for the differentiation between Parkinson's disease and atypical parkinsonian syndromes.<sup>1-5</sup>

PET imaging enables in vivo visualization and quantification of disease-specific radiotracer biodistributions in the patient's body. However, there are several parameters that affect the quality and quantitative accuracy of PET images, including positron range, the limited spatial resolution and resulting partial volume effect, contribution from scattered photons, photon attenuation, patient motion, and the image reconstruction algorithm. Attenuation of photons in vivo degrades the visual quality and quantitative accuracy of PET images, thereby adversely affecting interpretation and quantitation of activity concentration. Accurate attenuation correction is therefore mandatory in quantitative PET image reconstruction and plays a pivotal role in clinical PET scanning protocols. In stand-alone PET systems, attenuation correction is usually performed using either rod positron-emitting ( $^{68}\text{Ga}/^{68}\text{Ge}$ ) or point single-photon emitting ( $^{137}\text{Cs}$ ) sources orbiting around the patient. Since the energy of photons emitted from positron-emitting rod sources is the same and the  $\gamma$ -rays emitted by  $^{137}\text{Cs}$  (662 keV) are very close to the energy of annihilation photons in PET

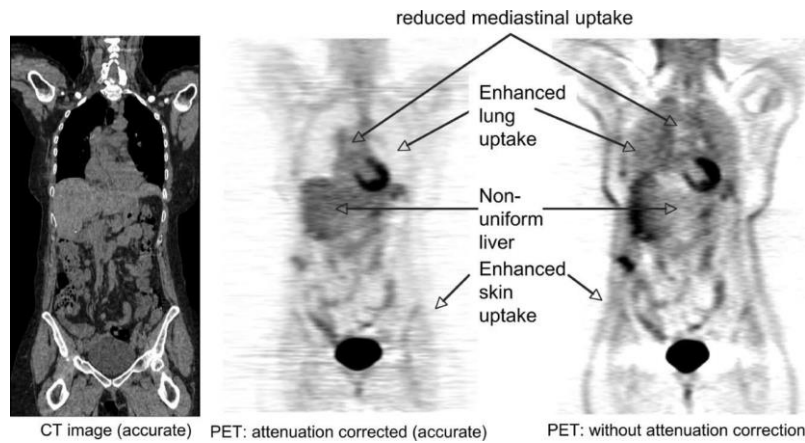


Fig. 2. CT and PET images showing the effects of photon attenuation in the PET emission data.<sup>6</sup>

(511 keV), transmission scanning-based attenuation correction is the method of choice for stand-alone PET scanners. In recent years, PET/CT scanners have gained widespread acceptance in the clinical setting since the availability of correlated functional and anatomical images was shown to improve the detection or staging of disease by highlighting areas of increased radiotracer uptake on the anatomical images, whereas regions that look abnormal in the anatomical image can draw attention to a potential area of disease where radiopharmaceutical uptake may be low (Fig. 2). In PET/CT systems, attenuation correction is achieved by X-ray transmission scanning using the CT sub-system of the combined unit. CT-based attenuation correction (CTAC) reduces substantially total scanning time and yields much lower statistical noise in the generated attenuation map ( $\mu$ -map) even when using low-dose CT scanning protocols. It also eliminates the need for rotating radionuclide transmission sources around the patient but suffers from many drawbacks, including the much higher radiation dose delivered to the patient compared to transmission scanning and the possibility brain PET

of producing artifacts in the attenuation corrected PET images, particularly in the presence of contrast agent and metallic objects in CT images. CT images display the distribution of attenuation coefficients within the patient's body at an effective energy ( $\sim 55\text{--}80$  keV) related to the generated X-ray spectra (80–140 kVp). Since the energy of the photons for the emission scan is 511 keV, reliable conversion methods are required to convert the attenuation coefficients (in Hounsfield units) acquired at the CT effective energy to linear attenuation coefficients ( $\mu$ ) at 511 keV. Another important issue is that CT uses a polychromatic X-ray spectrum whereas annihilation photons' energy in PET is monochromatic (511 keV). Hence, a conversion of the broad energy spectrum attenuation coefficients to linear attenuation coefficients at 511 keV is mandatory.<sup>6-8</sup>

In the last two years, convolution neural networks (CNNs) have outperformed the state of the art in many medical imaging tasks, such as image denoising, image reconstruction and end-to-end lesion detection.<sup>9-11</sup> However, CNN application for PET are more challenging than those for MR and CT due to the low resolution and noise characteristics of PET. This study aimed to investigate the feasibility of attenuation correction based on CNN technique in brain PET imaging without additional anatomical imaging. To reach this goal, a deep learning environment has been set up to create a CNN model, which was trained and tested by PET data obtained from both Monte Carlo simulation and real PET/CT scans. Based on our study results, several

suggestions have been made to improve the performance of deep learning based attenuation correction for brain PET imaging.

## 貳、研究方法與過程

### 一、深度學習模型

Deep learning model can learn a hierarchy of features, i.e., high-level features built upon low-level features. CNN is one popular type of deep learning models, in which trainable filters and local neighborhood pooling operations are applied in an alternating sequence starting with the raw input images. In the following, a CNN architecture for PET attenuation correction adopted from the model proposed by Nie et al. is described.<sup>12</sup> The training data for this CNN model consists of patches extracted from subjects with both uncorrected PET images and attenuation corrected PET images. The size of input (uncorrected) PET patch is  $32 \times 32$  and the size of output (corrected) PET patch is  $24 \times 24$ . The input and output patches are in correspondence, which means that they share the same center position in their aligned image space. To generate training samples for CNN, a large number of patches from uncorrected PET volume are extracted as inputs, and the corresponding corrected PET image patches are extracted as outputs. The total number of patches extracted from each volume is about 6000, which is sufficient to cover majority of the image volume.

In the CNN architecture, we first apply convolution with a filter size of  $7 \times 7$  on the input (uncorrected) PET patch to construct 32 feature maps in the first hidden layer. One voxel is padded along the first two dimensions. In the second layer, the outputs of the first layer are fed into another

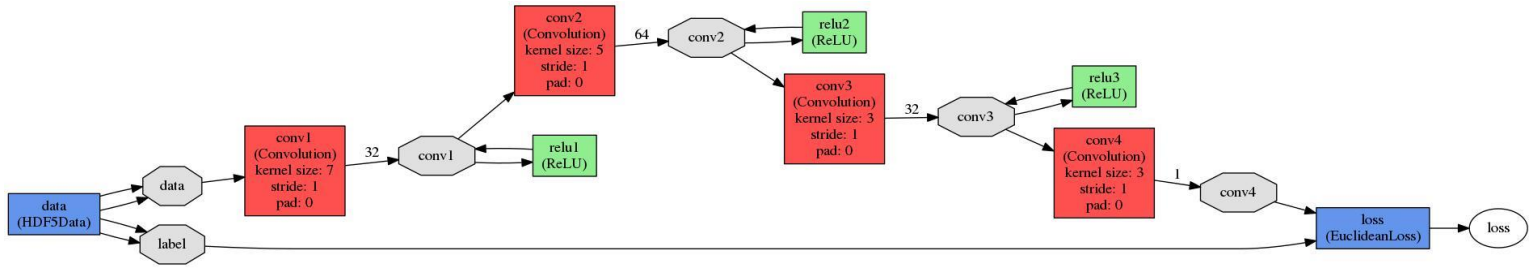


Fig. 3. The architecture for estimating attenuation corrected PET image from uncorrected PET image.

convolutional layer with 64 filters of size  $5 \times 5$ . The third convolutional layer contains 32 feature maps. Each of the feature maps is connected to all the input feature maps through filters of size  $3 \times 3$ . The output layer contains only one feature map generated by 1 filter of size  $3 \times 3$ , and it corresponds to the predicted (attenuation corrected) PET image patch. To keep the same image size, one voxel is padded along three dimensions in the last two layers. In all layers, we set stride as 1 voxel. The latent nonlinear relationship between uncorrected PET and attenuation corrected PET images is encoded by the large number of parameters in the network.

Caffe (Convolutional Architecture for Fast Feature Embedding) was modified to implement the architecture to minimize classification error and improves the directness and transparency of the hidden layer learning process.<sup>13</sup> Fig. 3 demonstrate the deep learning architecture, which was set up and drawn using Caffe. Caffe has command line, Python, and MATLAB interfaces for day-to-day usage, interfacing with research code, and rapid prototyping (Table 1).<sup>14</sup> While Caffe is a C++ library at heart and it exposes a modular interface for development,

Table 1. Comparison of deep learning libraries.<sup>14</sup>

Name	Caffe	MXNet	Torch	Deeplearning4j	Tensorflow	Theano	CNTK	Neon	Keras
Creator	UC Berkeley	CMU, UW and Microsot	Ronan Collobert et al.	SkyMind	Google	Universite de Montreal	Microsoft	Nervana System	Franois Chollet
Interface	C++, Python, MATLAB	C++, R, Python, Scala, Matlab, JavaScript, Go, Julia	Lua, LuaJIT, C	Java, Scala, Clojure	C++, Python, GO, Java	Python	NDL, C++, Python	Python	Python
Suitable model	CNN, RNN	CNN, RNN	DNN, CNN, RNN	DNN, CNN, RNN	DNN, CNN, RNN	DNN, CNN, RNN	CNN, RNN	DNN, CNN, RNN	DNN, CNN, RNN
OS	Linux, Win, OSX, Andr.	Linux, Win, OSX, Andr.	Linux, Win, OSX, Andr., iOS	Linux, Win, OSX, Andr.	Linux, OSX, Win	Linux, OSX, Win	Linux, OSX, Win	OSX, Linux	Linux, Win, OSX
Stars in github	20212	11170	7279	7203	68800	6914	12396	3200	19589
Multi-GPU	✓	✓	✓	✓	✓	×	✓	✓	×
Distributed	×	✓	×	✓	✓	×	✓	✓	×
Cloud computing	×	✓	×	×	✓	×	×	✓	×

not every occasion calls for custom compilation. The network parameters of CNN are updated by back-propagation using stochastic gradient descent algorithm. To train the network, the model hyper-parameters need to be appropriately determined. Specifically, the network weights are initialized by xavier algorithm, which can automatically determine the scale of initialization based on the number of input and output neurons. For the network bias, we initialize it to be 0. The initial learning rate and weight decay parameter are determined by conducting a coarse line search, followed by decreasing the learning rate during training. Both Monte Carlo simulation data and real patient data were used to train and test the CNN model for estimating attenuation corrected PET images from uncorrected PET images.

## 二、腦部 PET 成像系統之蒙地卡羅模擬

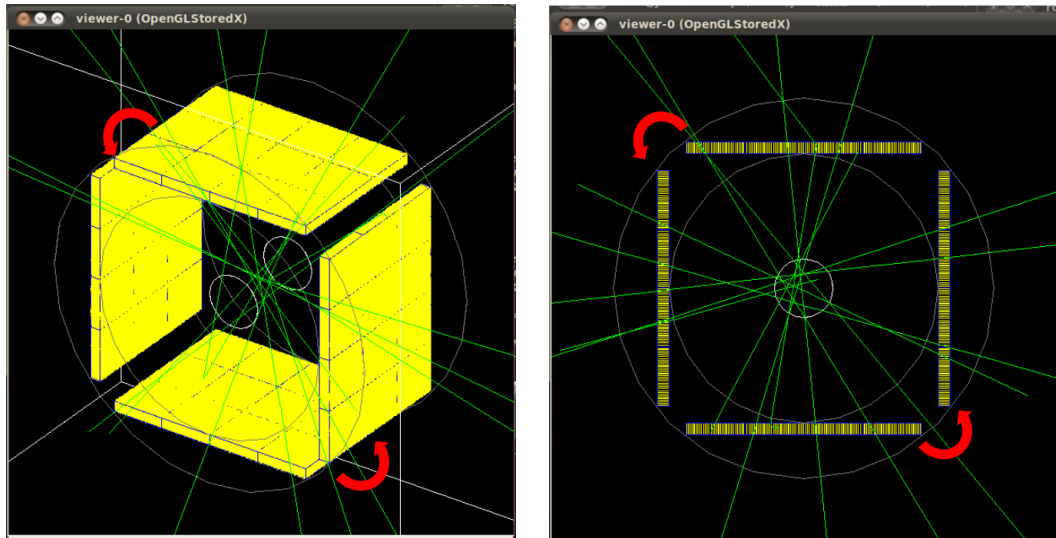


Fig. 4. Visualization of brain PET scanner modeled in GATE.

The GATE Monte Carlo toolkit based on the Geant4 code was used to simulate the brain PET system designed by Institute of Nuclear Energy Research (INER).<sup>15</sup> The brain PET system modeled in this study consists of two flat-panel type detectors at 180 degrees opposite each other. Each panel is made up of  $3 \times 4$  detector blocks, and each detector block contains  $31 \times 31$  pixelated array of  $1.51 \times 1.51 \times 10 \text{ mm}^3$  LYSO with a crystal pitch of 1.52 mm. The system covered an area of  $151 \times 201.4 \text{ mm}^2$ . The distance between two opposing detectors is 230 mm. The entire array is coupled with silicon photomultipliers (SiPMs) via a glass light guide. After data acquisition at the first angular position, the system rotated 90 degrees to the next angular position (Fig. 4). The simulated coincidence events from each angular position were stored in projection histogram with matrix size of  $11532 \times 11532$ .

In GATE simulation, a complete simulation script can be defined in

eight steps. The user needs to describe; (1) the camera geometry, (2) the phantom geometry, (3) the acquisition system (detector electronics response modeling), (4) the time parameters (acquisition start and stop times), (5) the data output format, (6) the physics processes, (7) the radioactive sources, and (8) the verbosity level. For each step, a specific macro was defined with standard GATE command lines. To describe a tomographic experiment, all components of the imaging device and the imaged object must be composed of elementary volumes. These volumes are arranged in a volume hierarchy where each volume possesses specific properties such as size, position, and material composition. The electromagnetic interactions used in GATE are derived from Geant4. The electromagnetic physics package manages electrons, positrons,  $\gamma$ -rays, X-rays, optical photons, muons, hadrons, and ions. Although GATE can simulate the physical process of positron source detection, 511-keV back-to-back photon source was used in this work in order to speed up simulation. To train the CNN model, PET data generated by simulating back-to-back photon source in water were used as the input data, while the corresponding label data were generated by simulating activity distribution of back-to-back photon source in vacuum. As in Geant4, GATE can use two different packages to simulate electromagnetic processes: the standard energy package, and the low energy package. In the standard energy package, photoelectric effect and Compton scatter can be simulated at energies above 10 keV. The low energy package extends the treatment of photons and electrons down to 250 eV and includes Rayleigh scattering. For biomedical applications,

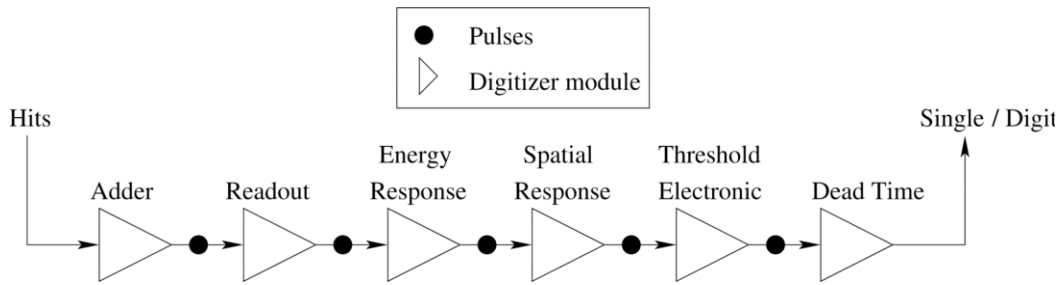


Fig. 5. The digitizer is organized as a chain of several modules that processes the hits to yield a single, which represents a physical observable.

the low energy package thus provides a more accurate model of the electromagnetic interactions. However, this comes at the price of increased computing time. In this work, the standard energy package was used to speed up simulation.

Digitization is the process of simulating the electronics response of a detector within a scanner. This involves the conversion of the charged particle and photon interactions into energy bins, detection positions, and coincidences. This is one of the key features in GATE that allows it to accurately simulate the behavior of real scanners. In order to do this, portions of the scanner geometry are designated as sensitive detectors, which record interactions within these regions. Next, the digitizer chain processes these recorded interactions and produces counts and coincidences. Sensitive detectors are used to store information about particle interactions (hereafter referred to as hits) within physical volumes. GATE only stores hits for those volumes that have a sensitive detector attached. All information regarding interactions within nonsensitive volumes is discarded. Two types of sensitive detectors are

defined in GATE: the crystal sensitive detector (crystalSD) and the phantom sensitive detector (phantomSD). The aim of the digitizer chain is to mimic a realistic detection process by building the physical observables from the hits. The observables of each detection event are the energy, position, and time of the interaction. The digitizer consists of a chain of processing modules that takes a list of hits from the sensitive detectors and transforms them into pulses referred to as singles (Fig. 5). To test the impact of different signal processing strategies, a simulation can be reprocessed with different digitizer chains using DigiGATE. At the end of a digitizer chain a coincidence sort can be added to find pairs of singles that are in coincidence. Pairs of singles can be considered coincidences whenever the time interval between the singles is less than a user-defined coincidence window. Each single is stored with its corresponding event number. If the event numbers of the singles associated in a coincidence are not the same, then it is a random coincidence. A similar flag exists for Compton scatters. Thus, the Compton scatter flag can be used to differentiate true from scattered coincidence pairs that have identical event flags. To exclude auto-coincidences of a particle interacting within several crystalSDs and hence resulting in several singles with the same event numbers, a user defined neighboring threshold can be used to reject coincidences of singles that are detected in nearby crystalSDs. Finally, multiple coincidences that correspond to more than two singles that are within the same coincidence window are discarded.

Table 2. Technical characteristics of the Discovery PET/CT 710 scanner.<sup>16</sup>

PET Detector	Specifications
Gantry dimensions (cm)	192 × 226.1 × 140
Weight (kg)	4,916
Patient port (cm)	70
Scintillator material	LBS (lutetium-based scintillator)
Scintillator dimensions (mm)	4.2 × 6.3 × 25
Crystal array per block	9 × 6
Number of detector rings	24
Number of crystals per ring	576
Number of crystals	13,824
Number of PMTs	1,024 (256 quad-anode)
Number of image planes	47
Axial field of view (cm)	15.7
Transaxial field of view (cm)	70
Slice overlap	User defined 1-23, Minimum recommendation 5 (10% overlap)
Image matrix sizes	128 × 128, 192 × 192, 256 × 256
Transmission source	CT attenuation correction
Vertical travel (cm)	2.5 – 20.5 below the isocenter
Acquisition modes	3D, 4D
Coincidence window (ns)	4.9
Lower energy threshold (keV)	425
Maximum axial coverage (cm)	170 – 200

### 三、 臨床病人腦部 PET/CT 掃描

Patient data were collected retrospectively from the Department of Nuclear Medicine at National Taiwan University Hospital. The institutional review board (IRB) has approved the protocol and issued a written notice of approval issued on October 16, 2019 (approval number: 201908077RIND). All patient data were acquired on a Discovery PET/CT 710 scanner (GE Healthcare, Milwaukee, USA). The technical specifications of the Discovery PET/CT 710 scanner are summarized in Table 2.<sup>16</sup> FDG PET/CT imaging was performed 45 min after injection

of FDG at a dose of 10 mCi for adult patients. Before FDG administration, subjects were asked to fast for at least 6 hours. Blood glucose level at the time of FDG injection was less than 150 mg/dL in all subjects. No additional glucose control drugs were used in subjects with high blood glucose levels. Sixty minutes after the administration of FDG, low-dose CT was performed for attenuation correction and precise anatomical localization. Thereafter, an emission scan was conducted in the three-dimensional mode. The average total PET/CT examination time was 15 minutes. The CT scan was obtained with tube voltage of 120 kVp and tube current of 50-150 mAs. The PET data were reconstructed by Vue Point Fx (6 iteration, 24 subsets) without and with CT-based attenuation correction. The uncorrected PET images were used as the input data to train the CNN model, while the corresponding label data were the PET images corrected for attenuation using CTAC.

#### 四、工作項目與執行時程

This project starts on September 29<sup>th</sup> and ends on December 31<sup>st</sup>. Because the deadline for uploading the final report is December 15<sup>th</sup>, the

Table 3. The Gantt chart describing the project works.

Month	9	10	11	12	
Working list					
Build up a brain PET simulator	■				Based on GATE
Set up deep learning environment	■	■			Based on Caffe
Apply for IRB application	■	■			Issued on 10/16
Generate simulation data		■	■	■	198 simulations
Collect real PET/CT scans			■	■	20 patient scans
Train and test CNN model			■	■	Running on CPU
Compose final report				■	Due by 12/15

actual duration is 3.5 months. Table 3 summarizes the progress of this project.

### 參、主要發現與結論

#### 一、研究結果

A 30-minute PET data acquisition for a spherical source with  $^{18}\text{F}$  activity of 670000 Bq embedded in a cylindrical phantom (10 cm in height) was

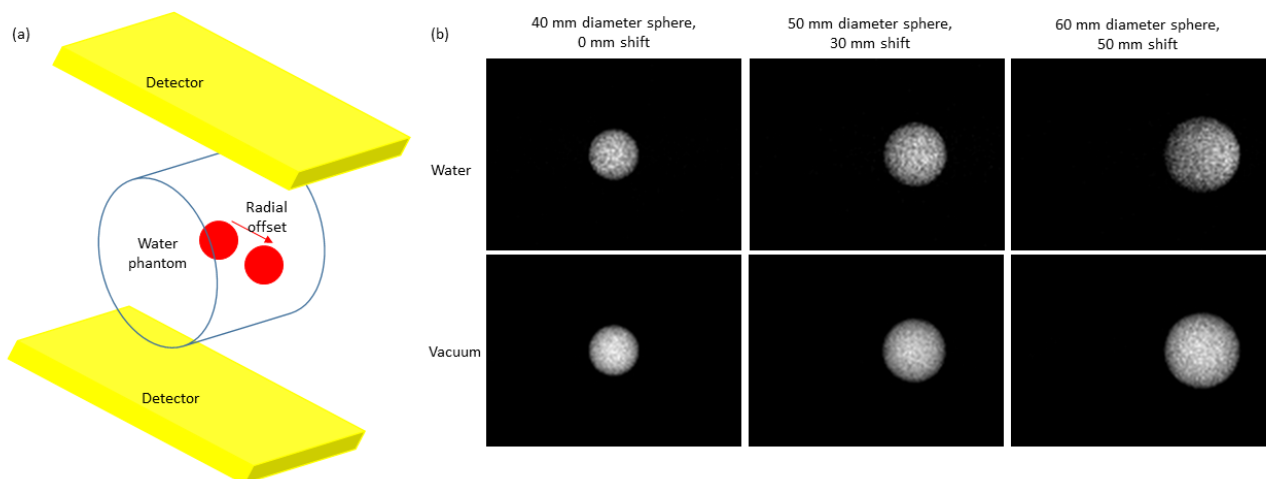


Fig. 6. (a) Illustration of geometry modeling in Monte Carlo simulation and (b) the simulated projections for spherical source in water (upper row) and in vacuum (lower row).

modeled in Monte Carlo simulation. Simulation was repeated using three different cylinder sizes (16, 18 and 20 cm in diameter), 2 different attenuation materials (water and vacuum), 3 different sphere sizes (40, 50, 60 mm in diameter), 11 different sphere locations (at center,  $\pm 1$  cm,  $\pm 2$  cm,  $\pm 3$  cm,  $\pm 4$  cm,  $\pm 5$  cm). Hence, a total of 198 simulations were performed. It takes 2 days to complete each simulation job. Fig. 6 shows the illustration of geometry modeling in Monte Carlo simulation and the simulated projections for spherical source in water and in vacuum. Fig. 7 shows the input data (spherical source in water) and the label data (spherical source in vacuum) generated from simulation and the output data from the CNN model. The CNN model has been trained for 3 weeks

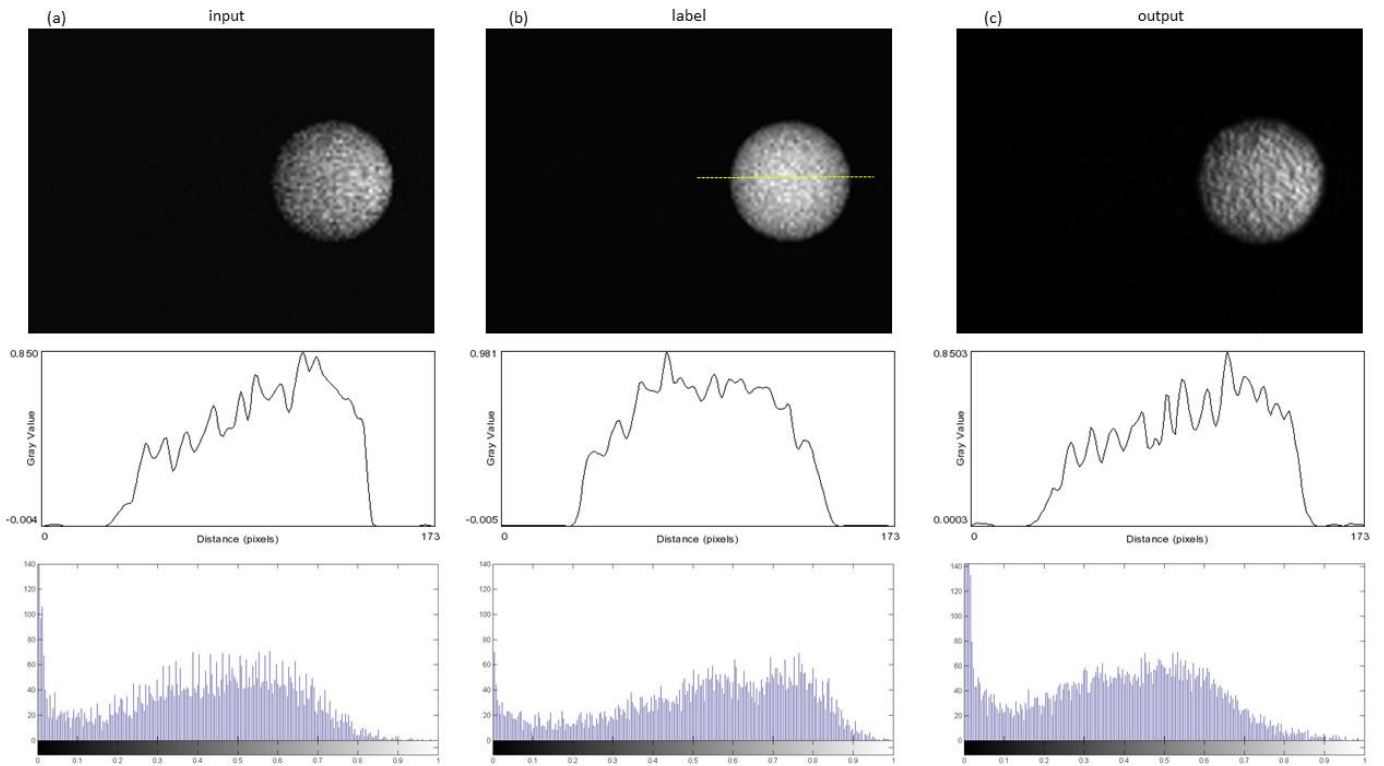


Fig. 7. (a) The input data and (b) the label data generated from simulation and (c) the output data generated by testing the CNN model (upper row: projection; mid row: intensity profile through the dash line; lower row: image histogram).

(forward/backward iteration 1254500). The intensity profile of output data in Fig. 7(c) is more flat than that for the input data, but the difference is little. Concerning the image histogram, the mean value of output data is higher than that for the input data, but is still lower than that for label data.

Our clinical brain dataset consists of 20 subjects, each with CT, uncorrected PET and attenuation corrected PET. Table 4 summarizes patient information of 20 real PET/CT scans. Fig. 8 demonstrate CT, uncorrected PET and attenuation corrected PET of brain in axial plane from 2 different patients. Fig. 9 shows the input data (uncorrected PET)

and the label data (attenuation corrected PET) from real patient scan and

Table 4. Patient information of 20 real PET/CT scans.

No.	Gender	Age	Diagnosis
1	M	79	Brain atrophy
2	F	19	Hashimoto's encenphalopathy
3	M	65	Left parietal ischemic stroke
4	F	23	Epilepsy
5	F	66	Brain atrophy
6	F	26	Suspected of autoimmune problems leading to dizziness and headache
7	M	73	Mild brain atrophy
8	M	75	Intracranial aneurysm and brain atrophy
9	F	23	Insufficient blood supply to the brain due to central nercous system damage
10	F	51	Patient falls, causes brain damage, decreases bilateral metabolism
11	F	64	Epilepsy
12	M	78	Dementia
13	M	59	Cerebral cavernous hemangioma
14	M	21	Drowsiness
15	F	34	Fever due to an unknown cause, FDG was performed and cerebellar blood flow was low
16	M	66	Demential
17	F	55	Parkinson's disease
18	F	70	Cortical basal ganglia degeneration, suspected due to waling impairment and cognitive decline
19	F	81	Mild cognitive impairment
20	M	56	Dementia

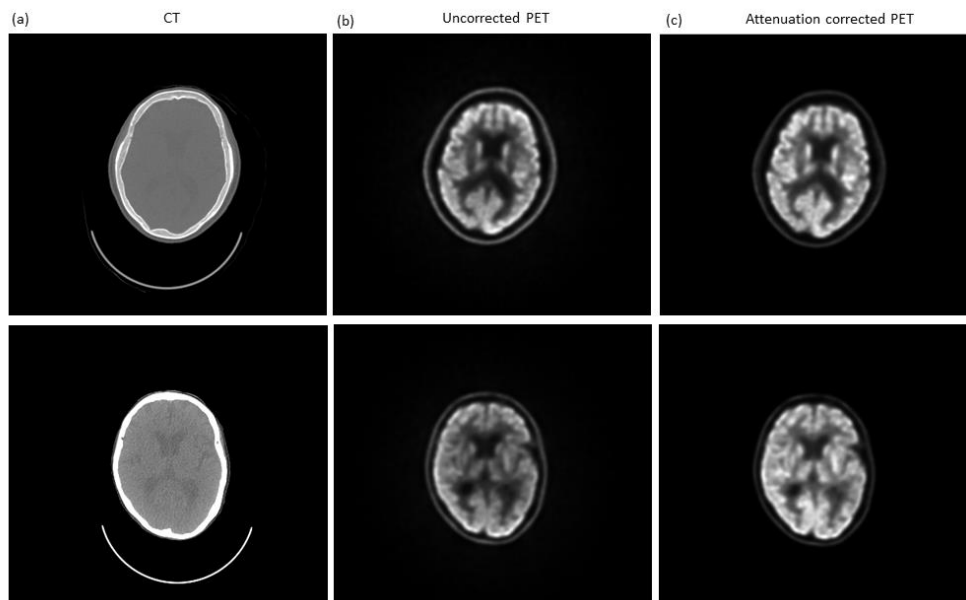


Fig. 8. (a) CT, (b) uncorrected PET and (c) attenuation corrected PET of brain in axial plane from 2 different patients.

the output data generated by testing the CNN model. The CNN model

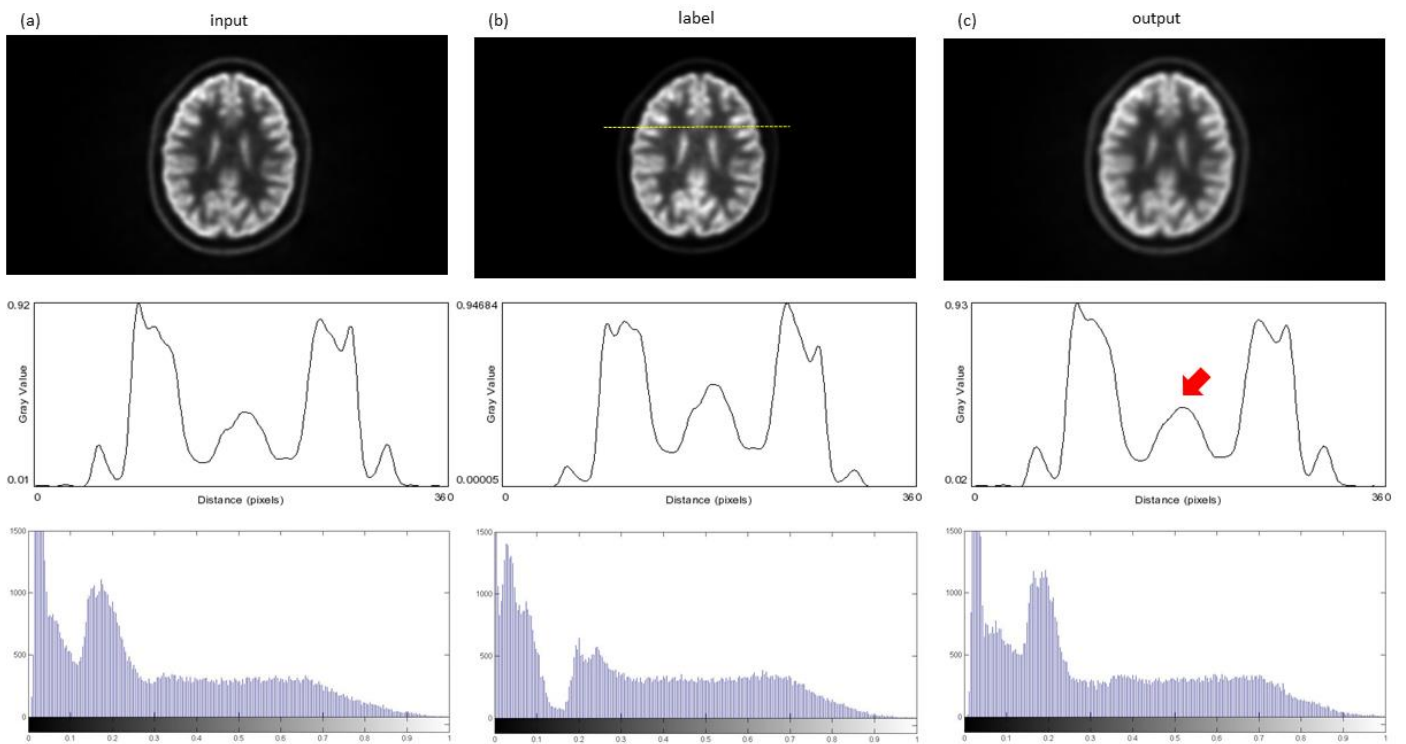


Fig. 9. (a) The input data and (b) the label data from real patient scan and (c) the output data generated by testing the CNN model (upper row: reconstructed image in the axial plane; mid row: intensity profile through the dash line; lower row: image histogram).

has the output data from the CNN model. The CNN model has been trained for 3 weeks (forward/backward iteration 1151500). For the output data in Fig. 9(c), the central portion of the intensity profile (red arrow) is higher than that for the input data, but the difference is not obvious compared to the label data. With regards to the image histogram of output data, the tendency of high intensity pixels is similar to that from label data, but not for the low intensity pixels.

## 二、 討論與建議

Based on our preliminary results, it was found that the performance of the CNN model investigated in this study is not acceptable. This

phenomenon is suspected to be related with several issues. First, a CNN model shown in Fig. 3 may be too simple for this work. PET generally has higher image noise than MRI and CT. Since complicated neural network models can integrate and absorb noise better than simple neural network models, a more complicated CNN model should be used to improve the performance of the output results. The deeply supervised nets method enforces direct and early supervision for both the hidden layers and the output layer by introducing companion objective to the individual hidden layers, which is used as an additional constraint to the learning process.<sup>17</sup> Fig. 10 demonstrate the modified CNN architecture for estimating attenuation corrected PET image from uncorrected PET image. The deeply supervised nets method can minimize classification error while making the learning process of hidden layers direct and transparent. It is expected that the CNN model with a deeply supervised feature can improve the performance of the output data. Second, the CNN model should be trained by using more image datasets to improve the performance of output data. The amount of training data plays a critical role in making the deep learning models successful. It has been well established both across industry and academia that for a given problem, with large enough data, a very different algorithms perform virtually the same. However, noisy labels inevitably degenerate the robustness of the learned model, especially for deep neural networks. The large data should have meaningful information and not just noise so that model can learn from it. Therefore, it is expected that if the CNN model is trained by using Monte Carlo simulation data generated with

voxelized brain phantom (Fig. 11) instead of the physical phantoms

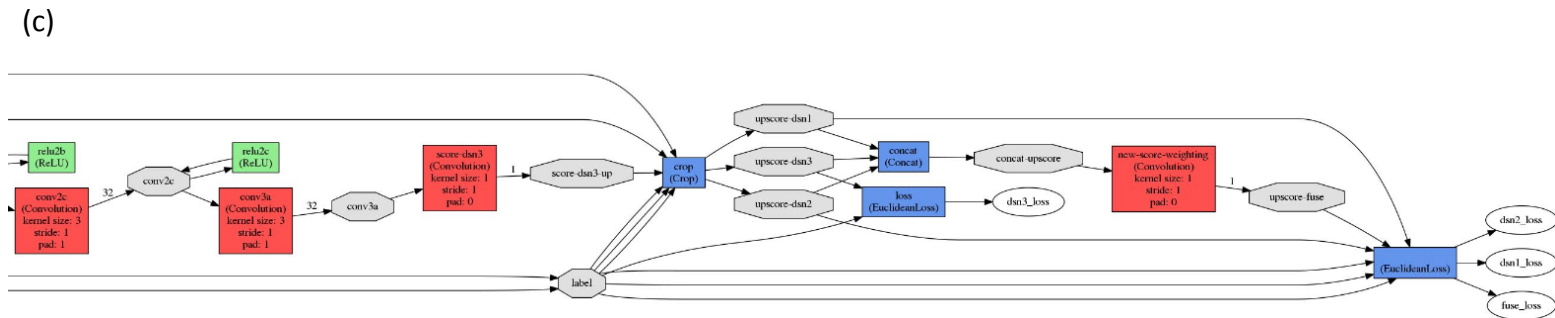
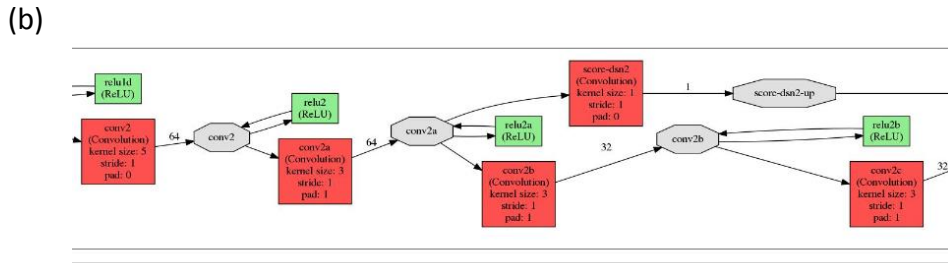
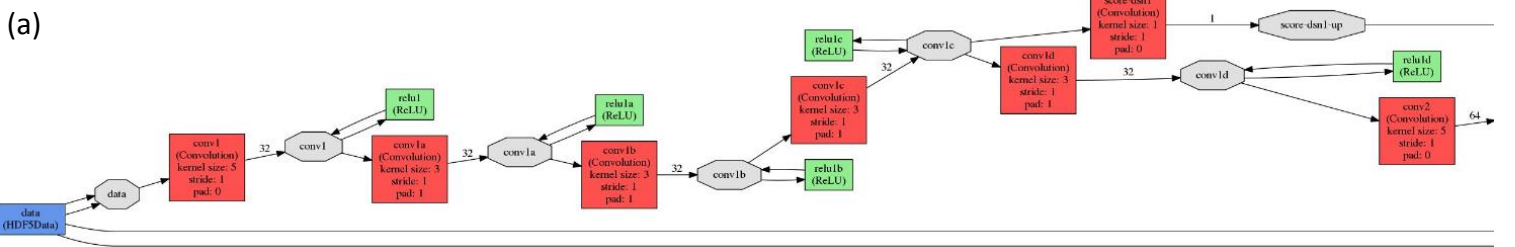
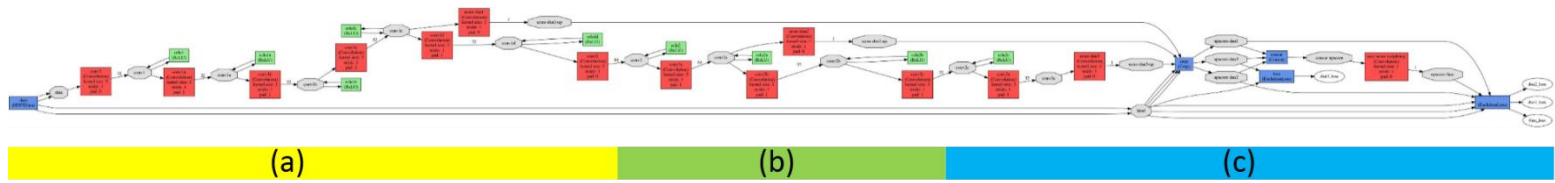


Fig. 10. The CNN architecture with a deeply supervised feature for estimating attenuation corrected PET image from uncorrected PET image. (a)-(c): partial enlarged CNN model.

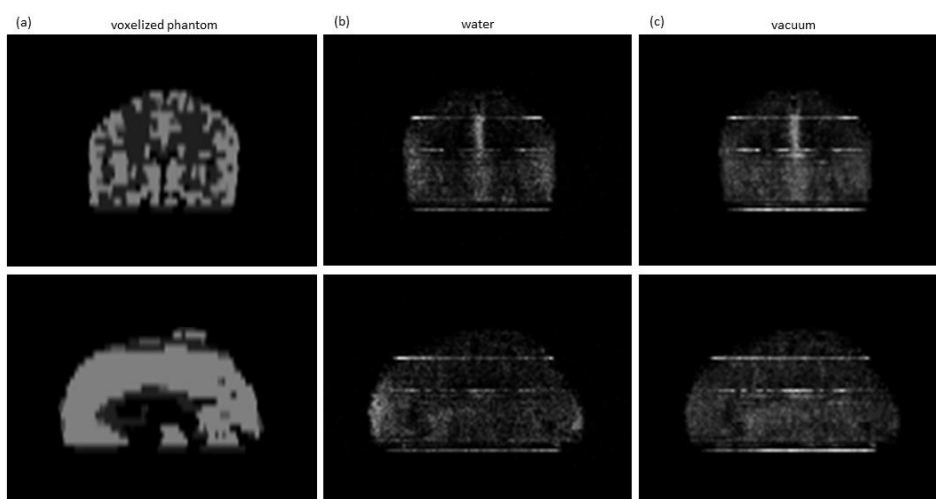


Fig. 11. (a) The voxelized brain phantom in coronal (upper) and sagittal planes (lower) and the simulated projections for the activity distribution of  $^{18}\text{F}$  in (b) water and (c) vacuum.

with simple geometry settings as conducted in this study, the performance of the CNN model could be improved. However, it takes about 2 weeks to complete the simulation job shown in Fig. 11(b) and 11(c). Third, when a 3D deep learning model is applied, the performance of the CNN output data could be improved. The CNN model used in this work is designed for 2D images, which may not be suitable for 3D volumetric images (i.e., MRI, CT and PET). Compared to 2D CNN, 3D CNN can better model the 3D spatial information due to the use of 3D convolution operations. 3D convolution preserves the spatial neighborhood of 3D image. As a result, 3D CNN can solve the discontinuity problem across slices, which are suffered by 2D CNN.

### 三、結論

For this project, we have accomplished the following works: (1) a Monte Carlo simulator based on GATE has been built to model the brain PET

system designed by INER; (2) 198 simulations have been conducted to train and test the CNN model; (3) IRB approval issued by National Taiwan University Hospital was obtained for this study; (4) 20 real PET/CT scans were collected to train and test the CNN model; (5) a deep learning environment based on Caffe has been set up; (6) a CNN model has been investigated for estimating attenuation corrected PET from uncorrected PET. Although the output data from the investigated CNN model have large discrepancy from the label data, these preliminary results give us valuable information concerning the simulation phantom type, the training data size, and the architecture of the CNN model. It is believed that the performance of the deep learning based attenuation correction for brain PET imaging can be substantially improved once the suggested modifications have been made.

## 肆、参考文献

1. Berti V, Pupi A, Mosconi L. PET/CT in diagnosis of movement disorders. *Annals of the New York Academy of Sciences*. 2011;1228:93-108.
2. Singhal T. Positron emission tomography applications in clinical neurology. *Seminars in neurology*. 2012;32(4):421-431.
3. Marcus C, Mena E, Subramaniam RM. Brain PET in the diagnosis of Alzheimer's disease. *Clinical nuclear medicine*. 2014;39(10):e413-422; quiz e423-416.
4. Tripathi M, Tripathi M, Damle N, et al. Differential diagnosis of neurodegenerative dementias using metabolic phenotypes on F-18 FDG PET/CT. *The neuroradiology journal*. 2014;27(1):13-21.
5. Spehl TS, Hellwig S, Amtage F, et al. Syndrome-specific patterns of regional cerebral glucose metabolism in posterior cortical atrophy in comparison to dementia with Lewy bodies and Alzheimer's disease--a [F-18]-FDG pet study. *Journal of neuroimaging : official journal of the American Society of Neuroimaging*. 2015;25(2):281-288.
6. Chen DL, Kinahan PE. Multimodality molecular imaging of the lung. *Journal of magnetic resonance imaging : JMRI*. 2010;32(6):1409-1420.
7. Lee TC, Alessio AM, Miyaoka RM, Kinahan PE. Morphology supporting function: attenuation correction for SPECT/CT, PET/CT, and PET/MR imaging. *The quarterly journal of nuclear medicine and molecular imaging : official publication of the Italian Association of Nuclear Medicine (AIMN) [and] the International Association of Radiopharmacology (IAR), [and] Section of the So*. 2016;60(1):25-39.
8. Buchbender C, Hartung-Knemeyer V, Forsting M, Antoch G, Heusner TA. Positron emission tomography (PET) attenuation correction artefacts in PET/CT and PET/MRI. *The British journal of radiology*. 2013;86(1025):20120570.
9. Munir K, Elahi H, Ayub A, Frezza F, Rizzi A. Cancer Diagnosis Using Deep Learning: A Bibliographic Review. *Cancers*. 2019;11(9).
10. Suzuki K. Overview of deep learning in medical imaging.

- Radiological physics and technology*. 2017;10(3):257-273.
11. Tajbakhsh N, Shin JY, Gurudu SR, et al. Convolutional Neural Networks for Medical Image Analysis: Full Training or Fine Tuning? *IEEE transactions on medical imaging*. 2016;35(5):1299-1312.
  12. Nie D, Cao X, Gao Y, Wang L, Shen D. Estimating CT Image from MRI Data Using 3D Fully Convolutional Networks. Paper presented at: Deep Learning and Data Labeling for Medical Applications; 2016//, 2016; Cham.
  13. Jia Y, Shelhamer E, Donahue J, et al. Caffe: Convolutional Architecture for Fast Feature Embedding. *arXiv e-prints*. 2014. <https://ui.adsabs.harvard.edu/abs/2014arXiv1408.5093J>. Accessed June 01, 2014.
  14. Zhang Z, Zhao Y, Liao X, et al. Deep learning in omics: a survey and guideline. *Briefings in functional genomics*. 2019;18(1):41-57.
  15. Jan S, Santin G, Strul D, et al. GATE: a simulation toolkit for PET and SPECT. *Physics in medicine and biology*. 2004;49(19):4543-4561.
  16. Yoon HJ, Jeong YJ, Son HJ, Kang D-Y, Hyun K-Y, Lee M-K. Optimization of the spatial resolution for the GE discovery PET/CT 710 by using NEMA NU 2-2007 standards. *Journal of the Korean Physical Society*. 2015;66(2):287-294.
  17. Lee C-Y, Xie S, Gallagher P, Zhang Z, Tu Z. Deeply-Supervised Nets. Proceedings of the Eighteenth International Conference on Artificial Intelligence and Statistics; 2015; Proceedings of Machine Learning Research.

附註

# 國立臺灣大學醫學院附設醫院D研究倫理委員會

Research Ethics Committee D

National Taiwan University Hospital

7, Chung-Shan South Road, Taipei, Taiwan 100, R.O.C

Phone: 2312-3456 Fax: 23951950

臨床試驗/研究許可書

許可日期：2019年10月16日

倫委會案號：201908077RIND

計畫名稱：深度捲積神經網路技術於頭部 PET 影像衰減校正之可行性研究。

試驗機構：國立臺灣大學醫學院附設醫院

部門/計畫主持人：核子醫學部 詹凱傑醫事放射師

上述計畫業經2019年10月14日本院D研究倫理委員會第93次會議審查同意，符合研究倫理規範，並同意使用回溯性病歷資料免除知情同意。本委員會的運作符合優良臨床試驗準則及政府相關法律規章。

本臨床試驗/研究許可書之有效期限為一年(自2019年10月16日至2020年10月15日止)，計畫主持人須依國內相關法令及本院規定通報嚴重不良反應事件及非預期問題，並應於到期日至少6週前提出持續審查申請表，本案需經持續審查，方可繼續執行。

主任委員



## Clinical Trial/Research Approval

Date of approval: Oct 16, 2019

NTUH-REC No. : 201908077RIND

**Title of protocol :** The feasibility of attenuation correction based on deep convolution neural network in brain PET imaging.

**Trial/Research Institution :** National Taiwan University Hospital

**Department/ Principal Investigator :** Department of Nuclear Medicine / Radiologist Jhan Kai jie

The protocol and the request for the waiver of informed consent for retrospective collection of medical records have been approved by the 93<sup>rd</sup> meeting of Research Ethics Committee D of the National Taiwan University Hospital on Oct 14, 2019. The committee is organized under, and operates in accordance with, the Good Clinical Practice guidelines and governmental laws and regulations.

The duration of this approval is one year (from Oct 16, 2019 to Oct 15, 2020). The investigator is required to report Serious Adverse Events and Unanticipated Problems in accordance with the governmental laws and regulations and NTUH requirements and apply for a continuing review not less than six weeks prior to the approval expiration date.

**Daniel Fu-Chang Tsai, M.D.**  
Chairman  
Research Ethics Committee D

